

Adiabatic transfer of amplitude using STIRAP-like protocols generalizes to many bipartite graphs

Koen Groenland,^{1,2,*} Carla Groenland,³ and Reinier Kramer⁴

¹*QuSoft, CWI, Science Park 123, 1098 XG Amsterdam, the Netherlands*

²*Institute of Physics, University of Amsterdam, Science Park 904, 1098 XH Amsterdam, the Netherlands*

³*Mathematical Institute, University of Oxford, Andrew Wiles Building, Radcliffe Observatory Quarter (550), Woodstock Road, Oxford OX2 6GG, United Kingdom*

⁴*Korteweg-de Vries Institute, University of Amsterdam, Science Park 107, P.O. Box 94248, 1095 GE Amsterdam, the Netherlands*

(Dated: April 7, 2022)

Adiabatic passage techniques, used to drive a system from one quantum state into another, find widespread application in physics and chemistry. We focus on the techniques called STImulated Raman Adiabatic Passage (STIRAP) and Coherent Tunnelling by Adiabatic Passage (CTAP), which employ a unique zero-energy eigenstate to transfer amplitude between ends of a linear chain. We find that many more general physical systems can use the same protocol, namely those with a (semi-)bipartite interaction graph which allows a perfect matching both when the sender is removed and when the receiver is removed. Many of the favorable stability properties of STIRAP/CTAP are inherited. We numerically test transfer between the leaves of a tree, and find surprisingly accurate transfer, especially when straddling is used. Our results open up new possibilities for coherent control and quantum state transfer in more general systems, and show that conventional STIRAP/CTAP is resilient to a large class of perturbations.

CONTENTS

I. Introduction	1
II. Conventional STIRAP	2
III. Generalizing STIRAP	2
IV. Applications	4
V. Simulations	4
VI. Conclusion	5
VII. Acknowledgments	5
References	5
i. Proofs of claims made in the main text	7
1. Proof of equivalence between 2a and 2b in Thm. 1	7
2. Dangling vertices do not affect the nullity	8
3. Graphs with certain matchings make our protocol work almost surely	8
ii. Robustness guarantees	9
iii. On the eigenvalue gap in generalized STIRAP	10
1. Interlaced eigenvalues	10
2. Numerical scaling	10

I. INTRODUCTION

Originally conceived as a scheme to transfer amplitude between the low-lying states of a Λ system, STImulated Raman Adiabatic Passage (STIRAP) [1] has proven to provide practical and high fidelity state manipulation due to the inherent stability to experimental imperfections [2]. It is now widely adopted in fields where accurate control of quantum states is vital, such as high precision measurement [3, 4], studies of atoms and molecules [5–9], and quantum information processing [10–14]. A closely related protocol, Coherent Tunnelling by Adiabatic Passage (CTAP) [15], is mathematically equivalent, but was proposed in the context of spatial transport of particles, such as electrons through nearby quantum dots or ultracold atoms through optical wells [16, 17].

With the advent of quantum information processing, accurate control in increasingly large systems has become an important scientific challenge [18]. The majority of work on CTAP and STIRAP focuses on either a small number of sites (typically 3) [2, 16], or extensions to larger systems that form a linear chain [15, 19]. Some notable exceptions are Refs. [20–24] which address different geometries, such as two- and even higher dimensional grids or branching trees. These protocols typically work through a clever mapping of such systems to the well-understood case of the 1D chain.

We present a completely different approach to find more general configurations that allow transfer protocols, by describing a system’s interactions in the language of graphs: the vertices represent basis states and edges represent interactions. We look at bipartite interactions, where the basis states can be separated into two sets, such that each state interacts only with states outside its own set. If the two sets differ in size by one, then

* Corresponding author, K.L.Groenland@cwi.nl

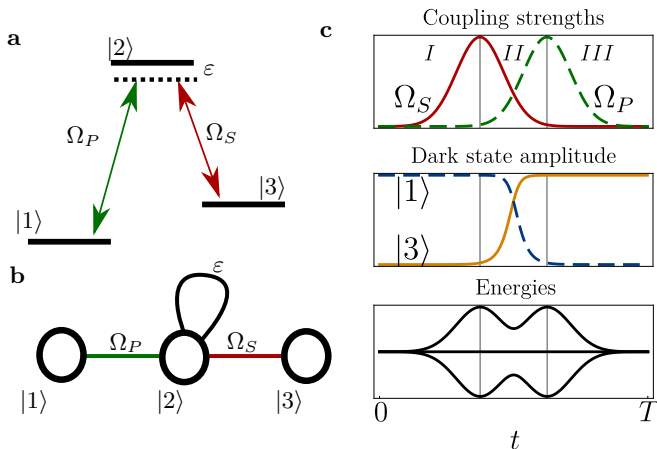


FIG. 1. The conventional STIRAP/CTAP protocol on a three-site Λ system. (a) The energy diagram of the three states, coupled by the Stokes (S) and Pump (P) lasers, also represented as a graph in (b). (c) Stacked plot showing the laser amplitudes, state amplitudes, and energies (eigenvalues λ) as a function of time, in arbitrary units. Stages I and III involve turning the couplings on/off, whereas stage II constitutes the relevant adiabatic driving part which transfers amplitude from state $|1\rangle$ to $|3\rangle$ as amplitudes Ω_S and Ω_P are slowly adjusted relative to each other.

amplitude transfer between states in the bigger set may be possible. We can guarantee successful transfer when certain graph properties are satisfied, as made precise in Thm. 1.

Interestingly, our treatment naturally provides a means to transfer amplitude to one out of multiple potential receivers, generalizing Ref. [22]. We find that the final state need not yet be known when starting the protocol, which could be an advantage in quantum information processing.

Our results advance the fields of STIRAP and CTAP in two ways. Firstly, they open the way to practical adiabatic passage in more general systems. Secondly, they shed light on possible perturbations in conventional STIRAP and their effect: we find that many perturbations, as long as they satisfy our assumptions, do not cause a qualitatively different effect on the state's evolution during the protocol.

Our work is closely related the field of perfect state transfer (PST), which addresses the same goal of transfer between two states $|a\rangle, |b\rangle$ in general graphs [25]. However, PST is concerned with *quenches* such that $|\langle b|e^{-iHt}|a\rangle| = 1$ for a time-independent Hamiltonian H . Therefore, PST is typically faster than adiabatic transfer, but it puts stringent constraints on the precise interaction strengths.

II. CONVENTIONAL STIRAP

The conventional protocol (Fig. 1) deals with a three-dimensional quantum system, consisting of eigenstates

$\{|j\rangle\}_{j=1}^3$ of some background Hamiltonian. To transfer amplitude from $|1\rangle$ to $|3\rangle$, a sequence of two laser pulses is applied: the Stokes pulse coupling $|2\rangle \leftrightarrow |3\rangle$, and the Pump pulse coupling $|1\rangle \leftrightarrow |2\rangle$. Throughout this work, we consider only the interaction picture and assume the rotating wave approximation to hold. The system's Hamiltonian then becomes

$$H(t) = \begin{pmatrix} 0 & \Omega_P(t) & 0 \\ \Omega_P(t) & \varepsilon & \Omega_S(t) \\ 0 & \Omega_S(t) & 0 \end{pmatrix}.$$

Here, $\Omega_{S/P}$ denotes the Rabi frequency (amplitude) of the Stokes and Pump lasers, respectively, and ε absorbs the off-resonances, assuming both are equal in size. One can check that one instantaneous eigenstate of H is the zero energy 'dark state' $|z\rangle$ given by

$$|z(t)\rangle = \frac{1}{\mathcal{N}} \begin{pmatrix} \Omega_P^{-1}(t) \\ 0 \\ -\Omega_S^{-1}(t) \end{pmatrix},$$

where \mathcal{N} denotes the normalization. Assuming that the relevant energy gaps are large compared to the time derivative of the Hamiltonian $\frac{d\Omega_{S/P}}{dt}$, the adiabatic theorem states that a system remains in its instantaneous eigenstates [26]. The dark state $|z\rangle$ has precisely the property that it transitions from $|1\rangle$ to $|3\rangle$ as Ω_S is gradually diminished while Ω_P is increased. Note the counter-intuitive order of the pulses, as indicated in Fig. 1. A key property of STIRAP is that the excited state $|2\rangle$ is never populated during this process, hence the protocol is independent of decoherence due to emission from this state. Thanks to this, and the inherent stability of adiabatic methods [27], the protocol is relatively stable to experimental imperfections, and is broadly adopted in practice [2].

III. GENERALIZING STIRAP

We observe that a key property of STIRAP/CTAP is the existence of a unique zero-energy eigenstate at all times, and that this state is localizable by lowering couplings incident to a particular site. This leads us to our main question: which other physical configurations pertain *precisely* one zero eigenvector, even when uncoupling a certain site?

We capture the more general configurations in the language of *weighted graphs* $G = (V, E, w)$. Here, the collection of vertices $V = \{|j\rangle\}_{j=1}^{\dim(\mathcal{H})}$ corresponds to a set of basis states of Hilbert space \mathcal{H} . Two vertices $v, u \in V$ are connected by an edge $(u, v) \in E$ if and only if an interaction that couples states $|u\rangle$ and $|v\rangle$ can be applied. The weights $w : E \rightarrow \mathbb{C}$ assign a complex amplitude to each of the interactions. Weights evaluated on non-existent edges are zero: $w_{uv} = 0$ for all $(u, v) \notin E$. The adjacency matrix A_G of a graph is then defined as the matrix of weights, with matrix elements $(A_G)_{uv} = w_{uv}$.

As long as we impose hermiticity through $w_{uv} = w_{vu}^*$, the control Hamiltonian H_G can be derived from a given graph G , through

$$H_G(t) = \sum_{u,v \in V} f_{uv}(t) w_{uv} |u\rangle\langle v|, \quad f_{uv}(t) = f_{vu}^*(t).$$

In this definition of the control Hamiltonian, we assume arbitrary time-dependent control over each allowed interaction, by tuning the controls $f_{uv}(t)$. We separate the interaction strengths into f and w because a clear distinction between graph properties and control fields is needed later.

The graph G from which H_G is derived will be called the *interaction graph*, which restricts the allowed interactions in H . Note that only systems whose interactions have a certain sense of resonance can be represented this way.

Thanks to the mapping to graphs, we can use various notions from graph theory. We denote with $G - v$ the graph G in which the vertex v and all the edges incident to v are removed. A *bipartite graph* has a vertex set V which can be separated into two independent subsets V_1, V_2 such that each edge $(u, v) \in E$ must run between V_1 and V_2 (that is, $u \in V_1$ and $v \in V_2$ or vice-versa). A *semi-bipartite graph* [28, 29] is a bipartite graph in which edges within V_2 are allowed (including self-loops), but edges within V_1 are still prohibited. For example, the graph in Fig. 1 is semi-bipartite with $V_1 = \{|1\rangle, |3\rangle\}$, but not bipartite unless $\varepsilon = 0$.

We are now ready to state our main result.

Theorem 1. *Let $G = (V, E, w)$ be a connected, weighted, semi-bipartite graph with parts V_1 and V_2 . Let $P = \{p_j\}_{j=1}^k \subseteq V_1$. Then, for any $a, b \in P$, there exists a control Hamiltonian $H_G(t)$ which adiabatically transfers amplitude from a to b , as long as the following holds:*

- 1 $|V_1| = |V_2| + 1$;

- 2 *Either of the following:*

- 2a For all p_j , $\det(A_{G-p_j}) \neq 0$;

- 2b A_G has a unique zero eigenvector, which has nonzero amplitude on each p_j .

Note that $\det(A) \neq 0$ implies that A does not have a zero eigenvalue. In the Supplemental Material, we show that requirements 2a and 2b are equivalent whenever 1 holds [30].

Requirement 2 is not very intuitive, but is virtually implied by a perfect matching. A graph contains a perfect matching whenever one can ‘marry’ pairs of vertices connected by an edge, such that all vertices are paired with precisely one partner. In the Supplemental Material, we prove that if $G - p_j$ allows such a perfect matching (for all $p_j \in P$), then upon choosing w_{uv} at random, requirement 2 is satisfied with probability 1. Moreover, a ‘dangling vertex’ which has just a single neighbor, can be added or

removed from the graph together with its unique neighbor, and doing so will not change the number of zero eigenvectors of the graph [30]. This allows straightforward generation of viable graphs with long-distance connectivity out of well understood basis graphs.

To prove Thm. 1, let us first show that requirement 1 implies the existence of a zero-energy eigenstate. For now, set $f_{uv} = 1$, such that $H_G = A_G$. Let \mathcal{V} denote the vector space spanned by the states corresponding to the vertices in V . Likewise, we use $\mathcal{V}_1, \mathcal{V}_2$ to denote the subspaces corresponding to subsets V_1, V_2 . We order the basis of \mathcal{V} by first stating the elements of \mathcal{V}_1 and then the elements of \mathcal{V}_2 . In this basis, the interaction graph has the form

$$A_G = \begin{pmatrix} 0 & B \\ B^T & C \end{pmatrix},$$

where B is a matrix of size $|V_1| \times |V_2|$ and C has size $|V_2| \times |V_2|$.

Thanks to $|V_1| = |V_2| + 1$, there must exist a zero-energy eigenvector $|z\rangle = (\vec{z}, \vec{0}) \in \mathcal{V}_1$ whose nonzero amplitudes \vec{z} are only located on sites in V_1 . This holds because in the eigenvalue equation,

$$\begin{pmatrix} 0 & B \\ B^T & C \end{pmatrix} \begin{pmatrix} \vec{z} \\ 0 \end{pmatrix} = \begin{pmatrix} 0 \\ B^T \vec{z} \end{pmatrix} = 0,$$

the system of equations $B^T \vec{z} = 0$ has $|V_1|$ variables and $|V_2|$ constraints, hence it must always have at least one non-trivial solution.

Importantly, $|z\rangle$ has many favorable stability properties. Its eigenvalue is *exactly* 0, independent of changes to w_{uv} , as long as the graph remains semi-bipartite. This makes the state’s dynamical phase easy to track. Moreover, it has exactly 0 amplitude on \mathcal{V}_2 , which makes it insensitive to any decoherence on sites in V_2 . The state $|z\rangle$ generalizes the ‘dark state’ of conventional STIRAP and CTAP, inheriting important features that make these protocols attractive for practical purposes.

In order for the adiabatic theorem to apply, we should guarantee that *no other* states with zero energy exist. We will give a simple choice of time-dependent controls $f_{uv}(t)$ that, given assumptions 1 and 2, satisfy

1. For $0 \leq t \leq T$, the state $|z(t)\rangle$ is the unique zero-energy eigenstate,
2. $H_G(0)|a\rangle = 0$, such that at time $t = 0$ the unique zero eigenstate is precisely the state $|z(0)\rangle = |a\rangle$,
3. $H_G(T)|b\rangle = 0$, such that at time $t = T$ the unique zero eigenstate is precisely the state $|z(T)\rangle = |b\rangle$.

A solution is as follows. We will assume that, for each vertex $v \in V_1$, the incident couplings are changed proportionally. Furthermore, we take all couplings within V_2 to be equal to one. Therefore, we set

$$\begin{aligned} f_{vu}(t) &= f_v(t) & \forall u \in V_2, v \in V_1; \\ f_{vu}(t) &= 1 & \forall u, v \in V_2. \end{aligned}$$

We will henceforth call such a setting ‘commensurate couplings’. This means that we can write

$$H_G(t) = F(t)A_G F^*(t), \quad (1)$$

where $F(t) = \text{diag}(f_1(t), \dots, f_{|V_1|}(t), 1, \dots, 1)$.

We then set

$$\begin{aligned} f_a(0) &= 0; \\ f_b(T) &= 0; \\ f_v(t) &\neq 0 \text{ for all } v \notin P; \end{aligned} \quad (2)$$

No two $f_v(t)$ may be zero simultaneously.

As long as all the f_v are non-zero, there is still a unique zero eigenvector of $H_G(t)$,

$$|z(t)\rangle \propto F(t)^{-1}|z\rangle,$$

as can be seen from Eq. 1. Because F is diagonal, $|z(t)\rangle$ is still located on V_1 . It is unique, because given any zero eigenvector $|w\rangle$ of $H_G(t)$, $F(t)|w\rangle$ is an eigenvector of A_G , hence must be equal, up to scaling, to $|z\rangle$.

Special care has to be taken when reducing weights to zero. When reducing f_p ($p \in P$) towards zero, assumption 2a guarantees that no zero eigenvectors occur on $G-p$, hence $|p\rangle$ must then be the unique zero eigenstate. Note that 2b also implies 2a [30].

This shows that any controls f_v satisfying Eq. 2 indeed pertain a unique zero-energy eigenstate, and provide the correct initial and final state at times $t = 0$ and $t = T$. The only couplings that actually *require* time-dependent control are those directly connected to sender and receiver; controlling any of the other couplings is optional. Moreover, the condition $\det(A_{G-p_j}) \neq 0$ guarantees that we can drop the requirement of commensurate couplings for a single p_j as long as all other sites remain commensurately coupled: the rank of A_G must be at least that of A_{G-p_j} , which shows that for *any* couplings between p_j and the rest of the graph, there can be at most one zero-energy state. Bringing all these couplings to zero must move this state to p_j . This freedom gives the protocol a convenient stability to imperfect controls when bringing the weights adjacent to p_j down to zero.

By the adiabatic theorem, a sufficiently high total time T allows state transfer at arbitrary accuracy. The time scale is determined by the gap in the spectrum around the zero eigenvalue, as opposed to the well-studied gap between the lowest and second lowest energy [31]. To our best knowledge, little is known about the gap around zero, and characterizing its scaling is an interesting open problem. Interestingly, we numerically find that the gap of most grids scales as $1/|V|$, but also find exceptions that decay faster than a polynomial in the graph size $|V|$ [30].

IV. APPLICATIONS

The mathematical framework we consider applies to various realistic cases, such as discrete electronic levels coupled by laser fields [2], electrons hopping through

quantum dots [15, 32], cold atoms or atomic condensates in optical potentials [17, 33, 34], or XX spin models in a single-excitation sector [35].

Our results show that CTAP and STIRAP work on many more systems than known previously. Moreover, decoherence mechanisms that can be turned into graphs which satisfy our assumptions should not have disrupting effects on the protocols. The most interesting application, however, might be in quantum information processing. Note that our protocols can transmit quantum information, for example when the transported state represents the position of a quantum particle with internal degrees of freedom, or when a superposition between a shared vacuum and an excitation on a graph may be made.

Ref. [36] observes that individual quantum processors based on quantum dots are limited in size, raising the need for communication between nearby processors. Our results readily generalize the CTAP protocol [15] to transfer electrons through a network of quantum dots, and the possibility to use more general graphs may be of great benefit for larger quantum computer architectures.

Another new application is in a delayed transfer scheme, previously addressed in Ref. [37]. The sender a can initialize the system into the dark state $|z\rangle$ and leave it at that, such that any party in P can retrieve the quantum state, at any time they like. This opens the possibility to share unclonable quantum information among many parties without yet knowing which party is required to obtain the information.

V. SIMULATIONS

As an example of the new possibilities in state transfer, we construct regular binary trees of depth k . To guarantee that requirement 1 is always fulfilled, we put another vertex on each edge (the white vertices), leading to graphs as shown in Fig. 2. The possible communicating parties P are chosen to be the leaves (endpoints) of the tree, allowing $|P| = 2^k$ parties to be connected. We choose a and b at maximum distance from each other.

We define the transfer error as $\mathcal{E} = 1 - |\langle b|U_T|a\rangle|$, where U_T denotes the unitary time-evolution operator as found by numerically solving Schrödinger’s Equation, and T is the total protocol’s time. We choose simple time-dependent couplings $f_a = Jt/T$ and $f_b = J(1 - t/T)$, while all other controls remain $f_v = 1$. Moreover, we define T^* as the lowest time for which $\mathcal{E} < 0.05$, setting a bar for transfer with 95% fidelity.

Owing to the exponentially large size $|V|$ of the graphs, the time required rapidly increases with k (Fig. 2). Interestingly, we find that the technique of straddling [15, 19], in which all controls f_v except for f_a and f_b are multiplied by a factor s , flattens the scaling down to roughly $T^* \approx 10\sqrt{k}$, up to a certain k where the steep increase is observed again. Although Ref. [38] already predicted a favorable scaling $T^* \propto \sqrt{n}$ for linear chains of length

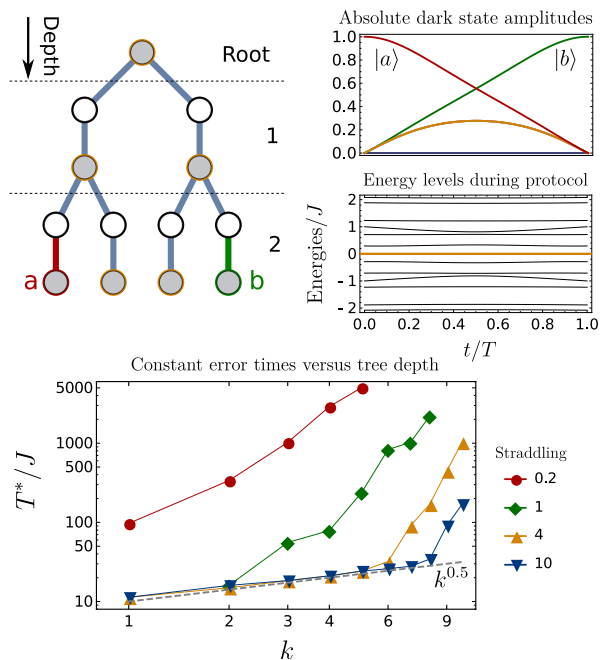


FIG. 2. Simulation results on tree graphs. A tree of depth $k = 2$ is shown on the top-left, with receivers a and b maximally separated. The top-right shows the ideal state evolution over time, and the energy levels during the protocol. The times T^* required for constant fidelity increase steeply with the exponential size $|V|$ of the graph (bottom), except when sufficiently strong straddling is applied, leading to $T^* \propto k^{0.5}$ (dashed line).

n in the strong straddling limit, it is surprising that in this case as similar better-than-linear scaling is found for much larger graphs, whose gap decays *exponentially* in k .

There are various reasons to believe that the strong

straddling scaling cannot remain valid for increasingly large systems, for example due to Lieb-Robinson bounds [39]. Still, with a modest straddling factor $s = 10$, transfer at favorable scaling $T^* \propto \sqrt{\log(|P|)}$ is observed for graphs of up to 1000 sites, showing that near-term experiments can benefit from this favorable scaling.

VI. CONCLUSION

To summarize, we extend the set of graphs in which STIRAP-like protocols are known to work. The sufficient requirements are made precise in assumptions 1 and 2. We inherit the most important properties of the conventional protocols: the adiabatic controls do not require precise amplitudes or timings, the system's energy is *exactly* zero at all times, and the fidelity is largely insensitive to decay on sites in V_2 . Various extensions, such as straddling and multi-party transfer, can be readily incorporated. In the studied example of tree-shaped graphs, we find that with mild straddling the fidelities are much better than naively expected.

As our requirements are sufficient but not necessary, we would be interested to see further work explore other graphs with unique zero eigenstates, and give guarantees on gap sizes for specific graphs. Moreover, we look forward to seeing state-of-the-art experiments test our results in practice.

VII. ACKNOWLEDGMENTS

We thank Andrew Greentree for inspiring discussion, and Kareljan Schoutens for discussions and feedback on the manuscript. R.K. was supported by VICI grant 639.033.211 of the Netherlands Organization for Scientific Research. K.G. was supported by the QM&QI grant of the University of Amsterdam, supporting QuSoft.

-
- [1] U. Gaubatz, P. Rudecki, S. Schiemann, and K. Bergmann. *Population transfer between molecular vibrational levels by stimulated Raman scattering with partially overlapping laser fields. A new concept and experimental results.* J. Chem. Phys., **92**, 9, 5363–5376 (1990). doi:10.1063/1.458514.
 - [2] N. V. Vitanov, A. A. Rangelov, B. W. Shore, and K. Bergmann. *Stimulated Raman adiabatic passage in physics, chemistry, and beyond.* Rev. Mod. Phys., **89**, 1, 015006 (2017). doi:10.1103/RevModPhys.89.015006.
 - [3] M. A. Kasevich. *Coherence with Atoms.* Science, **298**, 5597, 1363–1368 (2002). doi:10.1126/science.1079430.
 - [4] K. Kotru, D. L. Butts, J. M. Kinast, and R. E. Stoner. *Large-Area Atom Interferometry with Frequency-Swept Raman Adiabatic Passage.* Phys. Rev. Lett., **115**, 10, 103001 (2015). doi:10.1103/PhysRevLett.115.103001.
 - [5] P. Král, I. Thanopoulos, and M. Shapiro. *Colloquium: Coherently controlled adiabatic passage.* Rev. Mod. Phys., **79**, 1, 53–77 (2007). doi:10.1103/RevModPhys.79.53.
 - [6] S. Stellmer, B. Pasquiou, R. Grimm, and F. Schreck. *Creation of ultracold sr₂ molecules in the electronic ground state.* Phys. Rev. Lett., **109**, 11, 115302 (2012). doi:10.1103/PhysRevLett.109.115302.
 - [7] D. Petrosyan, D. D. B. Rao, and K. Mølmer. *Filtering single atoms from Rydberg-blockaded mesoscopic ensembles.* Phys. Rev. A, **91**, 4, 043402 (2015). doi:10.1103/PhysRevA.91.043402.
 - [8] S. A. Moses, J. P. Covey, M. T. Miecikowski, D. S. Jin, and J. Ye. *New frontiers for quantum gases of polar molecules.* Nature Physics, **13**, 1, 13–20 (2017). doi:10.1038/nphys3985.
 - [9] A. Ciamei, A. Bayerle, C.-C. Chen, B. Pasquiou, and F. Schreck. *Efficient production of long-lived ultracold*

- sr₂ molecules. *Phys. Rev. A*, **96**, 1, 013406 (2017). doi:10.1103/PhysRevA.96.013406.
- [10] J. Pachos and H. Walther. *Quantum Computation with Trapped Ions in an Optical Cavity*. *Phys. Rev. Lett.*, **89**, 18, 187903 (2002). doi:10.1103/PhysRevLett.89.187903.
- [11] F. Troiani, U. Hohenester, and E. Molinari. *High-finesse optical quantum gates for electron spins in artificial molecules*. *Physical Review Letters*, **90**, 20, 206802 (2003). doi:10.1103/PhysRevLett.90.206802.
- [12] E. Paspalakis and N. J. Kylstra. *Coherent manipulation of superconducting quantum interference devices with adiabatic passage*. *Journal of Modern Optics*, **51**, 11, 1679–1689 (2004). doi:10.1080/09500340408232482.
- [13] N. Timoney, I. Baumgart, M. Johanning, A. F. Varón, M. B. Plenio, A. Retzker, and C. Wunderlich. *Quantum gates and memory using microwave-dressed states*. *Nature*, **476**, 7359, 185–188 (2011). doi:10.1038/nature10319.
- [14] T. S. Koh, S. N. Coppersmith, and M. Friesen. *High-fidelity gates in quantum dot spin qubits*. *Proceedings of the National Academy of Sciences*, **110**, 49, 19695–19700 (2013). doi:10.1073/pnas.1319875110.
- [15] A. D. Greentree, J. H. Cole, A. R. Hamilton, and L. C. L. Hollenberg. *Coherent electronic transfer in quantum dot systems using adiabatic passage*. *Physical Review B*, **70**, 23, 235317 (2004). doi:10.1103/PhysRevB.70.235317.
- [16] R. Menchon-Enrich, A. Benseny, V. Ahufinger, A. D. Greentree, T. Busch, and J. Mompart. *Spatial adiabatic passage: A review of recent progress*. *Rep. Prog. Phys.*, **79**, 7, 074401 (2016). doi:10.1088/0034-4885/79/7/074401.
- [17] K. Eckert, M. Lewenstein, R. Corbalán, G. Birkel, W. Ertmer, and J. Mompart. *Three-level atom optics via the tunneling interaction*. *Phys. Rev. A*, **70**, 2, 023606 (2004). doi:10.1103/PhysRevA.70.023606.
- [18] J. Preskill. *Quantum Computing in the NISQ era and beyond*. *Quantum*, **2**, 79 (2018). doi:10.22331/q-2018-08-06-79.
- [19] V. S. Malinovsky and D. J. Tannor. *Simple and robust extension of the stimulated Raman adiabatic passage technique to N-level systems*. *Physical Review A*, **56**, 6, 4929–4937 (1997). doi:10.1103/PhysRevA.56.4929.
- [20] S. Longhi. *Coherent transfer by adiabatic passage in two-dimensional lattices*. *Annals of Physics*, **348**, 161–175 (2014). doi:10.1016/j.aop.2014.05.020.
- [21] C. J. Bradley, M. Rab, A. D. Greentree, and A. M. Martin. *Coherent tunneling via adiabatic passage in a three-well Bose-Hubbard system*. *Physical Review A*, **85**, 5, 053609 (2012). doi:10.1103/PhysRevA.85.053609.
- [22] A. D. Greentree, S. J. Devitt, and L. C. L. Hollenberg. *Quantum-information transport to multiple receivers*. *Physical Review A*, **73**, 3, 032319 (2006). doi:10.1103/PhysRevA.73.032319.
- [23] C. Batey, J. Jeske, and A. D. Greentree. *Dark State Adiabatic Passage with Branched Networks and High-Spin Systems: Spin Separation and Entanglement*. *Frontiers in ICT*, **2** (2015). doi:10.3389/fict.2015.00019.
- [24] B. Chen, W. Fan, Y. Xu, Y.-D. Peng, and H.-Y. Zhang. *Multipath adiabatic quantum state transfer*. *Phys. Rev. A*, **88**, 2, 022323 (2013). doi:10.1103/PhysRevA.88.022323.
- [25] C. Godsil. *State transfer on graphs*. *Discrete Mathematics*, **312**, 1, 129–147 (2012). doi:10.1016/j.disc.2011.06.032.
- [26] M. Born and V. Fock. *Beweis des Adiabatsatzes*. *Z. Physik*, **51**, 3, 165–180 (1928). doi:10.1007/BF01343193.
- [27] A. M. Childs, E. Farhi, and J. Preskill. *Robustness of adiabatic quantum computation*. *Phys. Rev. A*, **65**, 1, 012322 (2001). doi:10.1103/PhysRevA.65.012322.
- [28] K. Xu, R. Williams, S.-H. Hong, Q. Liu, and J. Zhang. *Semi-bipartite Graph Visualization for Gene Ontology Networks*. In D. Eppstein and E. R. Gansner (editors), *Graph Drawing*, Lecture Notes in Computer Science, pages 244–255. Springer Berlin Heidelberg (2010). ISBN 978-3-642-11805-0.
- [29] O. Al-Kofahi and A. Kamal. *Network coding-based protection of many-to-one wireless flows*. *Selected Areas in Communications, IEEE Journal on*, **27**, 797–813 (2009). doi:10.1109/JSAC.2009.090619.
- [30] . *Supplementary Material [to be inserted by publisher]*.
- [31] A. E. Brouwer and W. H. Haemers. *Spectra of Graphs* (2012).
- [32] T. Hensgens, T. Fujita, L. Janssen, X. Li, C. J. Van Diepen, C. Reichl, W. Wegscheider, S. Das Sarma, and L. M. K. Vandersypen. *Quantum simulation of a Fermi-Hubbard model using a semiconductor quantum dot array*. *Nature*, **548**, 7665, 70–73 (2017). doi:10.1038/nature23022.
- [33] E. M. Graefe, H. J. Korsch, and D. Witthaut. *Mean-field dynamics of a Bose-Einstein condensate in a time-dependent triple-well trap: Nonlinear eigenstates, Landau-Zener models, and stimulated Raman adiabatic passage*. *Phys. Rev. A*, **73**, 1, 013617 (2006). doi:10.1103/PhysRevA.73.013617.
- [34] I. Bloch, J. Dalibard, and S. Nascimbène. *Quantum simulations with ultracold quantum gases*. *Nature Physics*, **8**, 4, 267–276 (2012). doi:10.1038/nphys2259.
- [35] T. Ohshima, A. Ekert, D. K. L. Oi, D. Kaslizowski, and L. C. Kwek. *Robust state transfer and rotation through a spin chain via dark passage*. arXiv:quant-ph/0702019 (2007).
- [36] L. M. K. Vandersypen, H. Bluhm, J. S. Clarke, A. S. Dzurak, R. Ishihara, A. Morello, D. J. Reilly, L. R. Schreiber, and M. Veldhorst. *Interfacing spin qubits in quantum dots and donors—hot, dense, and coherent*. *npj Quantum Information*, **3**, 1, 34 (2017). doi:10.1038/s41534-017-0038-y.
- [37] K. Groenland. *Adiabatic state distribution using anti-ferromagnetic spin systems*. *SciPost Physics*, **6**, 1, 011 (2019). doi:10.21468/SciPostPhys.6.1.011.
- [38] A. D. Greentree, J. H. Cole, A. R. Hamilton, and L. C. L. Hollenberg. *Scaling of coherent tunneling adiabatic passage in solid-state coherent quantum systems*. In J.-C. Chiao, D. N. Jamieson, L. Faraone, and A. S. Dzurak (editors), *Smart Materials, Nano-, and Micro-Smart Systems*, page 72. Sydney, Australia (2005). doi:10.1117/12.583193.
- [39] E. H. Lieb and D. W. Robinson. *The finite group velocity of quantum spin systems*. *Commun.Math. Phys.*, **28**, 3, 251–257 (1972). doi:10.1007/BF01645779.
- [40] M. Mitzenmacher and E. Upfal. *Probability and computing*. Cambridge University Press (2017).
- [41] C. R. J. R. A. Horn. *Matrix Analysis*. Cambridge University Press (1985).

Appendix i: Proofs of claims made in the main text

1. Proof of equivalence between 2a and 2b in Thm. 1

Let us recall Thm. 1:

Theorem 1. *Let $G = (V, E, w)$ be a connected, weighted, semi-bipartite graph with parts V_1 and V_2 . Let $P = \{p_j\}_{j=1}^k \subseteq V_1$. Then, for any $a, b \in P$, there exists a control Hamiltonian $H_G(t)$ which adiabatically transfers amplitude from a to b , as long as the following holds:*

- 1 $|V_1| = |V_2| + 1$;

- 2 *Either of the following:*

- 2a For all p_j , $\det(A_{G-p_j}) \neq 0$;

- 2b A_G has a unique zero eigenvector, which has nonzero amplitude on each p_j .

In this section, we will prove that assumptions 2a and 2b are equivalent under the assumption of 1. More precisely, we prove the following proposition.

Proposition 2. *Let $G = (V, E, w)$ be a weighted, semi-bipartite graph with parts V_1 and V_2 , such that $|V_1| = |V_2| + 1$, and let $p \in V_1$. Then the following are equivalent:*

- a $\det(A_{G-p}) \neq 0$;

- b A_G has a unique zero eigenvector, which has non-zero amplitude on p .

Proof. We start with the implication from *a* to *b*. By the start of the proof of Thm. 1, we know that A_G has at least one zero eigenvector, so the rank of A_G can be at most $|V| - 1$. However, as $\det(A_{G-p}) \neq 0$, it must be of maximal rank, which is also $|V| - 1$. As the rank of a submatrix gives a lower bound on the rank of a matrix, this shows that $\text{rk } A_G \geq |V| - 1$. Therefore, there is a unique zero eigenvector.

Let this eigenvector be v , let its component at p be v_p , and its components away from p be \tilde{v} (so \tilde{v} is a vector with $|V| - 1$ components). We can write A_G as a block matrix

$$A_G = \begin{pmatrix} 0 & b_p \\ b_p^T & A_{G-p} \end{pmatrix},$$

where we wrote the component p as the first component for simplicity. As v is a zero eigenvector, we get

$$0 = A_G v = \begin{pmatrix} 0 & b_p \\ b_p^T & A_{G-p} \end{pmatrix} \begin{pmatrix} v_p \\ \tilde{v} \end{pmatrix} = \begin{pmatrix} b_p \tilde{v} \\ b_p^T v_p + A_{G-p} \tilde{v} \end{pmatrix}.$$

If now $v_p = 0$, then $\tilde{v} \neq 0$, as an eigenvector cannot be zero, but then $A_{G-p} \tilde{v} \neq 0$, as $\det(A_{G-p}) \neq 0$. This is a contradiction, so we must have $v_p \neq 0$.

Now we prove the implication from *b* to *a* by contrapositive. Hence we assume $\det(A_{G-p}) = 0$, and show that there exists a zero eigenvector of A_G whose p -component is zero. Again, for notational simplicity, we write the component p as the first component, so we have

$$A_G = \begin{pmatrix} 0 & B \\ B^T & C \end{pmatrix} = \begin{pmatrix} 0 & 0 & b_p \\ 0 & 0 & \tilde{B} \\ b_p^T & \tilde{B}^T & C \end{pmatrix}.$$

From this, we get

$$A_{G-p} = \begin{pmatrix} 0 & \tilde{B} \\ \tilde{B}^T & C \end{pmatrix},$$

where, crucially, the sizes of \tilde{B} and C are equal by the assumption $|V_1| = |V_2| + 1$. Hence,

$$\det(A_{G-p}) = \pm \det(\tilde{B} \tilde{B}^T) = \pm \det(\tilde{B})^2.$$

Now, by assumption $\det(A_{G-p}) = 0$, so $\det(\tilde{B}^T) = 0$. Therefore, there exists a zero eigenvector u of \tilde{B}^T . If we define $v = (0, u, 0)$, then

$$A_G v = \begin{pmatrix} 0 & 0 & b_p \\ 0 & 0 & \tilde{B} \\ b_p^T & \tilde{B}^T & C \end{pmatrix} \begin{pmatrix} 0 \\ u \\ 0 \end{pmatrix} = \begin{pmatrix} 0 \\ 0 \\ \tilde{B}^T u \end{pmatrix} = 0,$$

so we have constructed a zero eigenvector of A_G with zero amplitude on p , giving a contradiction. \square

Remark 3. In fact, the implication from a to b goes through even in the case G is not semi-bipartite; the proof does not use this assumption. However, for the other direction, it is essential.

2. Dangling vertices do not affect the the nullity

For an $(n \times n)$ -matrix A , let $\eta(A) = n - \text{rk}(A)$ denote the nullity of the matrix.

Lemma 4. *Let G be a graph with a vertex v of degree 1. Let u be the unique neighbor of v . Then*

$$\eta(A_G) = \eta(A_{G-\{v,u\}}).$$

Proof. Let \tilde{G} denote the graph $G - \{v, u\}$. Assuming for convenience that v and u are the first and second column of the adjacency matrix A_G respectively, we can write

$$A_G = \begin{pmatrix} 0 & w_{uv} & 0 \\ w_{vu} & w_{uu} & b \\ 0 & b^t & A_{\tilde{G}} \end{pmatrix}.$$

We can write any vector α as $(\alpha_v, \alpha_u, \tilde{\alpha})$. Now $w_{uv} \neq 0$ and

$$0 = A_G \alpha = \begin{pmatrix} 0 & w_{uv} & 0 \\ w_{vu} & w_{uu} & b \\ 0 & b^t & A_{\tilde{G}} \end{pmatrix} \begin{pmatrix} \alpha_v \\ \alpha_u \\ \tilde{\alpha} \end{pmatrix}$$

imply that $\alpha_u = 0$, $\alpha_v = -\frac{1}{w_{vu}} b \cdot \tilde{\alpha}$, and $A_{\tilde{G}} \tilde{\alpha} = 0$. Hence, we get a linear isomorphism $\ker A_G \rightarrow \ker A_{\tilde{G}}: (\alpha_v, \alpha_u, \tilde{\alpha}) \mapsto \tilde{\alpha}$ with inverse $\tilde{\alpha} \mapsto (-\frac{1}{w_{vu}} b \cdot \tilde{\alpha}, 0, \tilde{\alpha})$. As the nullity is the dimension of the kernel, this shows $\eta(A_G) = \eta(A_{\tilde{G}})$. \square

3. Graphs with certain matchings make our protocol work almost surely

A perfect matching in a graph G is a set of disjoint edges that covers all the vertices.

Theorem 5. *Let $G = (V, E, w)$ be a weighted semi-bipartite graph with parts V_1 and V_2 where $|V_1| = |V_2| + 1$. Let $P = \{p_j\}_{j=1}^k \subseteq V_1$. Suppose that for all i there exists a perfect matching in $G - p_i$. Then, if weights w_{uv} are chosen uniformly at random from $[0, 1]$ for all $uv \in E$, we find $\det(A_{G-p_j}) \neq 0$ for all p_j with probability 1.*

Note that the theorem exactly gives us condition (2a) required by the protocol.

Proof. It suffices to prove that $\det(A_{G-p_i}) \neq 0$ with probability 1 for a fixed $i \in \{1, \dots, k\}$; the claim of the theorem then follows since a countable intersection of events with probability 1 still has probability 1.

Let $p = p_i$ be given. We will first permute the rows and columns of the matrix A_{G-p} to bring it in a convenient form; such a permutation only affects the determinant of the matrix by a sign, which is irrelevant to us.

By assumption, there is a perfect matching on the graph $G - p$. Since $|V_1 - p| = |V_2|$ and there are no edges within V_1 , any perfect matching must use only edges between V_1 and V_2 . Let $u_1 v_1, \dots, u_k v_k \in E \cap (V_1 \times V_2)$ denote the edges given in a perfect matching on $G - p$. Permute the rows and columns such that the rows are in the order $u_1, v_1, u_2, v_2, \dots$ and the columns are in the order $v_1, u_1, v_2, u_2, \dots$. We show with an inductive argument that for all $\ell \in \{1, \dots, k\}$, the matrix A_ℓ on the first 2ℓ rows and columns has non-zero determinant with probability 1. This proves the claim.

For $\ell = 1$, we consider

$$\det \begin{pmatrix} w_{u_1 v_1} & 0 \\ w_{v_1 v_1} & w_{u_1 v_1} \end{pmatrix} = w_{u_1 v_1}^2,$$

since $w_{u_1 u_1} = 0$ as $u_1 \in V_1$. As $w_{v_1 v_1}$ is sampled uniformly at random from $[0, 1]$, this is non-zero with probability 1. Now suppose we have shown the statement up to some ℓ . We find

$$\det \begin{pmatrix} A_\ell & b_1 & b_2 \\ d_1 & w_{u_{\ell+1} v_{\ell+1}} & 0 \\ d_2 & w_{v_{\ell+1} v_{\ell+1}} & w_{u_{\ell+1} v_{\ell+1}} \end{pmatrix} = \det(A_\ell) w_{u_{\ell+1} v_{\ell+1}}^2 + b w_{u_{\ell+1} v_{\ell+1}} + c$$

for some b and c which do not depend on $w_{u_{\ell+1} v_{\ell+1}}$, and where we may assume that $\det(A_\ell) \neq 0$. Since the other entries do not depend on $w_{u_{\ell+1} v_{\ell+1}}$ and this gets sampled independently of the other entries, we may view $\det(A_\ell)$, b and c as constants. Since there are at most two possible values in $[0, 1]$ which make a quadratic polynomial $ax^2 + bx + c$ equal to zero (if $a \neq 0$), with probability 1 the expression will be non-zero. Continuing until $\ell + 1 = k$, we conclude $\det(A_{G-p}) \neq 0$ with probability 1 as desired. \square

Remark 6. From the proof of the theorem, it follows that various of the assumptions in the theorem can be relaxed: the only requirement is that the weights are chosen from a continuous distribution (in the sense that any particular value has probability 0) and this requirement is only necessary for the edges involved in the matching.

In fact, it is possible to show that the adjacency matrix of G is equivalent to a matrix with non-zero entries on the diagonal if and only if there is a perfect matching. Limited generalisation is also possible to non-bipartite graphs.

Appendix ii: Robustness guarantees

A lower bound on the determinants $\det(A_{G-p_i})$ gives the robustness guarantee that our protocol will keep working even if the weights cannot be held exactly at the aimed value. More precisely, if $|\det(A_{G-p_i})| > \epsilon$ for some $\epsilon > 0$, then by continuity of the determinant, this remains true even if the entries of A_{G-v} (that is, the weights on the edges) get permuted by at most some δ . Since the determinant is a polynomial, we may expect δ to be of a similar scale to ϵ . This implies that the uniqueness of the zero eigenvector would be guaranteed even if the weights of the edges are slightly perturbed. Note that the weights on the edges adjacent to p_i do not affect the determinant at all.

The proof of Theorem 5 extends to give a weak lower bound on the determinant.

Theorem 7. *Let G be a semi-bipartite graph on vertex classes V_1 and V_2 with a perfect matching $u_1 v_1, \dots, u_\ell v_\ell$. Suppose the weights on some edges of G , including the $w_{u_i v_i}$, are chosen independently and uniformly at random from $[0, 1]$. Then with probability at least $(\frac{1}{2})^\ell$, we have $|\det(A_G)| > (\frac{1}{2})^{3\ell-1}$.*

Proof. We may assume there are no edges within V_1 . (This assumption can be left out but makes the analysis easier.) As in the proof of Theorem 5, we reorder the columns to $u_1, v_1, u_2, v_2, \dots$ and the rows to $v_1, u_1, v_2, u_2, \dots$ and prove the claim for all submatrices A_ℓ spanned by the first 2ℓ rows and columns for all $\ell \in \{1, \dots, k\}$.

The statement is true for $\ell = 1$: $\det(A_1) = w_{u_1 v_1}^2 > \frac{1}{4}$ with probability at least $\frac{1}{2}$. Suppose now that $|\det(A_\ell)| \geq (\frac{1}{2})^{3\ell-1}$ with probability at least $(\frac{1}{2})^\ell$ for some ℓ . Again, we find

$$\det \begin{pmatrix} A_\ell & b_1 & b_2 \\ d_1 & w_{u_{\ell+1} v_{\ell+1}} & 0 \\ d_2 & w_{v_{\ell+1} v_{\ell+1}} & w_{u_{\ell+1} v_{\ell+1}} \end{pmatrix} = \det(A_\ell) w_{u_{\ell+1} v_{\ell+1}}^2 + b w_{u_{\ell+1} v_{\ell+1}} + c$$

takes the form $ax^2 + bx + c$, where a, b, c do not depend on $x = w_{u_{\ell+1} v_{\ell+1}}$ and can hence be viewed as constants by the independence assumption, and where $|a| \geq (\frac{1}{2})^{3\ell-1}$ with probability at least $(\frac{1}{2})^\ell$.

We can rewrite $ax^2 + bx + c = a(x + b')^2 + c'$ for possibly different values b', c' . Then $|a(x + b')^2 + c'| \leq (\frac{1}{2})^{3(\ell+1)-1}$ if and only if $a(x + b')^2 \in \left(-c' - (\frac{1}{2})^{3(\ell+1)-1}, -c' + (\frac{1}{2})^{3(\ell+1)-1}\right)$. The probability of this happening is maximized when $b' = -\frac{1}{2}$, $|c'| = (\frac{1}{2})^{3(\ell+1)-1}$ and the sign of c' and a are different; we may assume $a > 0$ as the other case goes analogous. In this case the interval is $\left(0, 2(\frac{1}{2})^{3(\ell+1)-1}\right) = \left(0, (\frac{1}{2})^{3\ell+1}\right)$. We find $a \geq (\frac{1}{2})^{3\ell-1}$ with probability at

least $(\frac{1}{2})^\ell$, in which case independently with probability $\frac{1}{2}$ we have $|x + b'| \geq \frac{1}{2}$. Hence with probability at least $(\frac{1}{2})^{\ell+1}$, we find

$$a(x + b')^2 \geq \left(\frac{1}{2}\right)^{3\ell-1} \left(\frac{1}{2}\right)^2 = \left(\frac{1}{2}\right)^{3\ell+1} \notin \left(0, \left(\frac{1}{2}\right)^{3\ell+1}\right). \quad \square$$

We cannot hope to do much better than the result above. Consider the case in which $A = \text{diag}(a_1, a_1, \dots, a_k, a_k)$ is a diagonal matrix, such that $\det(A) = a_1^2 \cdots a_k^2$ where the a_i get chosen independently and uniformly at random. Using the law of large numbers or the Central Limit Theorem and the fact that $-\log(U(0, 1)) \sim \text{Exp}(1)$, it follows that $a_1 \cdots a_k$ is concentrated around $(\frac{1}{e})^k$. In fact, one can prove using Chernoff bounds [40] that

$$\mathbb{P}\left(a_1 \cdots a_k \geq \left(0.5^{2/3}\right)^k\right) \leq e^{-(1/144)k}.$$

Hence without further assumptions, we cannot hope to improve the exponential decay in the lower bound of the theorem.

Appendix iii: On the eigenvalue gap in generalized STIRAP

The eigenvalue gap between the ground state and first excited state is an active field of research. However the gap between a zero eigenvalue and the nearest non-zero eigenvalue seems to have received significantly less interest. Below, we share our preliminary findings on the gap around eigenvalue 0.

1. Interlaced eigenvalues

When matrix entries get chosen from $[0, 1]$, all eigenvalues satisfy $|\lambda| \leq d_{\max}(G)$ for $d_{\max}(G)$ the maximum degree of G . Since the determinant is the product of the eigenvalues, this gives the lower bound $|\lambda| \geq \frac{\det(A_G)}{d_{\max}(G)^{n-1}}$ for a graph G on n vertices. We can obtain a lower bound on the eigenvalue gap using the following well-known result, which follows from the fact that A_{G-p} is a principal submatrix of A_G [41].

Theorem 8 (Cauchy interlacing theorem). *Let G be a graph with a vertex p . Let $\lambda_1 \leq \dots \leq \lambda_{n+1}$ be the eigenvalues of A_G and $\mu_1 \leq \dots \leq \mu_n$ the eigenvalues of A_{G-p} . Then*

$$\lambda_1 \leq \mu_1 \leq \lambda_2 \leq \mu_2 \leq \dots \leq \lambda_n \leq \mu_n \leq \lambda_{n+1}.$$

In our set-up, one of the λ_i will be equal to 0, and the theorem shows that that the gap to the second absolutely smallest eigenvalue is at least $\min_i |\mu_i|$, and hence the eigenvalue gap

$$\Delta(G) \geq \max_{p \in V_1} \min_{\mu \text{ eigenvalue of } G-p} |\mu|.$$

Along with the bounds on $\det(A_{G-p})$ from the previous section, we can use this to obtain a lower bound on the eigenvalue gap of G . This bound is very weak, and based on the experiments outlined below it is our expectation that vastly better bounds can be obtained.

2. Numerical scaling

Fig. 3 depicts the scaling of the energy gap around the zero energy state, as a function of the number of vertices $|V|$, for various types of graphs. For most graphs, we considered the unweighted versions, setting $w_{uv} = 1$ whenever the corresponding edge is present. Some graphs have the annotation ‘random’, which means that the graphs typically do not have a unique zero eigenvalue when all weights equal one; using our results we can ensure the existence of a unique zero eigenvalue by multiplying each weight w_{uv} with a random number chosen independently and uniformly from between 0 and 2. We took the average energy gap over 50 such perturbations.

These results show that the energy gap often decays roughly as $\Delta E \propto |V|^{-1}$ or better, similarly to conventional STIRAP over a linear chain, with hexagonal grids being an exception.

The precise details of the graph generation is as follows.

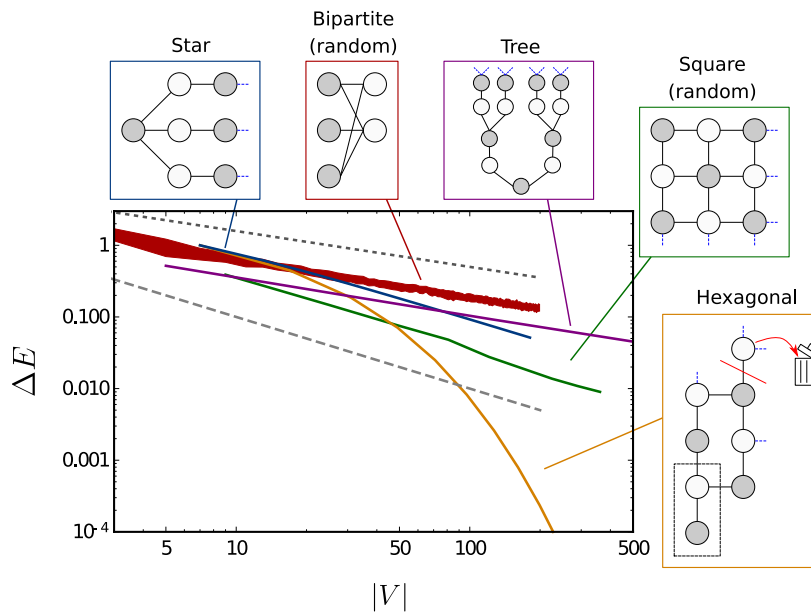


FIG. 3. Scaling of the eigenvalue gap ΔE between the unique zero eigenvalue and the closest other eigenvalue, on a log-log scale. These are calculated for various bipartite graphs of various sizes $|V|$. The annotation (random) indicates that the weights were randomly chosen in the interval $(0,2)$ to guarantee a unique zero eigenvector. The lower dashed line indicates $\Delta E = 1/|V|$, and the upper dashed line follows $\Delta E = 10/\sqrt{|V|}$. Interestingly, for most of the graphs we study, the gaps decay scales proportional to $1/|V|$ or better. Hexagonal grids are an exception, as these are found to decay superpolynomially.

We generate *star graphs* by connecting k ‘arms’, linear chains of length m , to a single center vertex. Interestingly, the eigenvalue gaps do not change as the number of arms increases. We fix the number of arms to 3 and vary the chain lengths to make larger graphs.

The *hexagonal grids* consist of unit cells of size 2. We take k^2 copies of these unit cells and place them on a $k \times k$ square grid, which is connected as indicated in Fig. 3. To enforce an odd number of sites, we remove a single site in the top-right corner, leading to $2k^2 - 1$ sites in total. Interestingly, the hexagonal grids are the only graph configuration we considered whose gap decays superpolynomially (yet slower than an exponential). Randomly perturbing weights does not change this behavior.

The *square grids* are chosen to have k by k vertices, where k is an odd number.

The *bipartite graphs* consist of two parts of size $m+1$ and m , respectively. Each potential edge which can be laid to connect the two parts is added with probability $p = 0.81$. Because these graphs are also random, for each datapoint, we also averaged the gap size over 50 random instantiations of the edge set. The thickness of the line indicates the standard deviation.

Lastly, the subdivided binary *trees* are generated as in the main text: starting from a complete binary tree of certain depth, we create an additional vertex on each edge, which makes sure that $|V_1| = |V_2| + 1$.